Acta Odontologica Scandinavica, 2012; 70: 133–139

informa
healthcare

ORIGINAL ARTICLE

Three-dimensional analysis of the pulp cavity on surface models of molar teeth, using X-ray micro-computed tomography

MERETE MARKVART[1], LARS BJØRNDAL[1], TRON A. DARVANN[2], PER LARSEN[2,3], MICHEL DALSTRA[4] & SVEN KREIBORG[2,3]

[1]*Department of Cariology and Endodontics, School of Dentistry, Faculty of Health Sciences, University of Copenhagen, Copenhagen, Denmark,* [2]*3D Craniofacial Image Research Laboratory (School of Dentistry, University of Copenhagen, Copenhagen University Hospital: Rigshospitalet; and DTU Informatics, Technical University of Denmark), Copenhagen, Denmark,* [3]*Department of Pediatric Dentistry and Clinical Genetics, School of Dentistry, Faculty of Health Sciences, University of Copenhagen, Copenhagen, Denmark, and* [4]*Department of Orthodontics, School of Dentistry, Faculty of Health Sciences, University of Aarhus, Aarhus, Denmark*

Abstract

Aim. The purpose of this study was to investigate the scanning and segmentation precision of surface models of molars for the detection of small volumes, such as the reduced pulp cavity; formation of mineral deposits; detection of narrow root canals and to improve the clinical and morphological understanding of the number of root canals and their configuration. ***Methods.*** Eighteen human molars were scanned using X-ray micro-computed tomography. The reconstruction of the surface models had a precision of <1 voxel, using three-dimensional software and quantitative color mapping. In order to relate the measurements to changes over time the size of the pulp chambers was classified in two well-defined groups. ***Results.*** The mineral deposits were more evenly distributed in small pulp chambers than in large, but complete root canal calcification was never observed. No difference was observed in the material with respect to the presence of intra-radicular connections. In upper molars, a second mesiobuccal canal (mb_2) frequency of 91% was found. The difference in length between the first mesiobuccal canal (mb_1) and mb_2 was <1 mm. The number of root canals could be related to the number of root cones. ***Conclusion.*** In summary, three-dimensional surface models were made with a high precision; an increased accumulation of mineral deposits was noted in molars with small pulp chambers and combined with the consistent pattern of intra-radicular connections, the potential endodontic treatment complexity is underlined in such cases. Finally, an improved understanding of root canal prevalence was reached, when merging well-defined definitions on root morphology and clinical classification systems.

Key Words: *endodontics, micro-computed tomography, pulp cavity, root canal morphology, root cone*

Introduction

Detailed information about root canal anatomy is essential in endodontics [1] and clinical classification systems have been developed to describe various root canal configurations [2]. The use of X-ray micro-computed tomography (Micro-CT) scanning has facilitated *in vitro* analysis of the internal and external root morphology [3–5], including the evaluation of root canal preparations after instrumentation [5–13] and broad software applications [14]. On the basis of Micro-CT data, it should be possible to further improve the morphological understanding of established clinical root classification systems [2,15], as consensus is still needed. In this context, invasive and non-invasive methods have shown that the mb_2 prevalence in maxillary permanent molars varies from 18.6–95.2% [16–20]. The reported variation in root canal prevalence may be related to the clinical level of magnification [18] and the basic macrostructures building up the root canal system in terms of root cones and separation structures [21–24]. Moreover, if three-dimensional (3D) reconstructed surface models are used for the evaluation of narrow root canals, the

Correspondence: Merete Markvart, DDS, PhD research assistant, Department of Cariology and Endodontics, School of Dentistry, Faculty of Health Sciences, University of Copenhagen, Nørre Allé 20, DK-2200 Copenhagen N, Denmark. Tel: +45 35 32 68 11. Fax: +45 35 32 65 05. E-mail: merma@sund.ku.dk

(Received 28 October 2010; revised 20 February 2011; accepted 31 March 2011)

ISSN 0001-6357 print/ISSN 1502-3850 online
DOI: 10.3109/00016357.2011.600707

scanning and segmentation precision is crucial for the evaluation of small volumes such as the second mesiobuccal canal (mb_2). A recent Micro-CT study analyzed the root canal system in the mesiobuccal root component of the first permanent maxillary molar [25] and found that the prevalence of the mb_2 was rather low: 65.2%. In addition, calcified segments in the root canals were visualized. Since magnification tools such as the operating microscope have become so prevalent and are even covered in undergraduate textbooks [26], more data about the reduced pulp cavity are required. The formation of secondary dentin in the pulp cavity after complete development of the tooth crown is a well known parameter in estimation of age [27]. In addition, older molar teeth have revealed formation of irregular and atubular dentin upon the mesial aspect of the floor of the pulp chamber [28]. In light of this the size of the pulp chambers may act as an indicator on changes over time. The aims in this study were: (i) to examine the scanning and segmentation precision of surface models of human molars for the potential detection of small volumes, (ii) to examine morphological aspects of mineral deposits in the pulp cavity of varying sizes, including the mb_2 prevalence and length in maxillary permanent molars and (iii) to improve the general understanding of root canal configurations using established definitions of root morphology and clinical classification systems.

Materials and methods

Sample material

X-rays were taken with a parallel technique from a batch of freshly extracted molars to select intact molars with varying sizes of the pulp cavity. The teeth were from a Danish population and had been extracted for reasons unrelated to the present study (mainly due to periodontal disease). We selected 11 maxillary and seven mandibular molar teeth without major destructions, and kept them in 0.5% aqueous chloramine. The roots were embedded in Epofix Kit (Struers A/S, Copenhagen, Denmark).

Scanning, segmentation and surface modeling

The teeth were scanned using a μ CT40 Microtomography scanner (SCANCO Medical AG, Brüttisellen, Switzerland). The molars were placed upright and scanned perpendicular to their longitudinal axes at standard resolution (250 projections per 180°), with a pixel size, slice thickness and slice increment of 30.7 μm. The scanner operated at 55 kV and 72 μA. The total number of slices per tooth varied between 589–769. The slices were imported into Analyze7.0 (AnalyzeDirect, Inc., Stilwell, KS) and median filtering was performed in order to eliminate noise. The objects were segmented semi-automatically and polygonal surface models were produced from each data set (Micro-CT image volume) using *Landmarker* version 2.0.3 [29].

Scanning and segmentation precision

The scanning precision was determined by re-scanning one tooth after re-positioning but with otherwise identical scanner settings. 3D surface models were created from both scans [30], employing the same intensity threshold, and these were subsequently spatially registered to each other [31]. For each surface point p on one of the models, the distance d_p to the closest location on the surface of the other model was determined and the overall precision was defined as the mean of these distances.

The segmentation precision was determined by repeating the segmentation process twice for 18 different data sets. Surface models were created from each segmentation and d_p was determined for each segmentation pair. Each tooth was sectioned into 100 axial slices, thereby providing an anatomical correspondence for the same slice in all teeth. For each slice in each tooth, a mean d_p was calculated by averaging the d_p values of all points within that slice and the average of these values in the sample of 18 pairs was taken as an overall segmentation precision for each slice. Finally, the overall segmentation precision was defined as the mean precision for all 100 slices. Range and standard deviation were determined for the scanning and segmentation precision using IDL (Interactive Data Language, version 7.1, ITT Visual Information Solutions, CO 80301, USA).

We applied a quantitative symmetric color scale to visualize d_p between two surface models of the same tooth. The color scale is symmetric around zero (green) and ranges from −30.7 μm (blue) to 30.7 μm (red). The segmentations were also used to develop resin models with different morphology. Two-colored stereo lithography (stl) models were prepared, scaled 4:1 in size (Prototal AB, Instrumentvägen 6, SE-553 02 Jönköping, Sweden).

Qualitative and quantitative morphological analysis of the pulp cavity

The size of the pulp cavity was used as an indicator of changes over time [28]. The size of the pulp chamber was measured centrally and the sizes were classified into two groups: (a) distance >1 mm between the roof and the furcal wall; (b) distance ≤1 mm. The distribution of mineral deposits was examined with respect to groups a and b as well as tooth type using the definition previously described by Park et al. [25]. The presences of mineral deposits in the pulp cavity were detected not as secondary dentine but as calcified segments connected to the walls of the pulp cavity

or as separated objects. The mean difference in canal length between the first mesiobuccal canal (mb_1) and mb_2 was calculated on the basis of the center of each root canal.

For the morphological description of the root canal complex, the definitions used were previously described by Carlsen and Alexandersen [21–24]:

- The root component is composed of 1–3 macro morphological units (root cones), which can be separated either completely or incompletely by inter-radicular projections or root grooves (Figure 1).
- A primary main canal is located centrally in a root complex, a separated root component, or a separated root cone (Figures 1A and B).
- A secondary main canal is located centrally in either a non-separated root component or a non-separated root cone (Figure 1C).
- The intra-radicular connection/canal connects two secondary main canals; the lateral canal connects the internal cavity with the outer surface of the root complex.

For the clinical description of root canal types, the following canal configuration was defined by Vertucci [15]:

- Type 1 has a single root canal from orifice to apex;
- Type 2 has two canals that combine and exit as one at the apex;
- Type 3 has one canal at the orifices that divides, recombines and exits as one at the apex;
- Type 4 has two root canals from orifices to apex;
- Type 5 has one canal at the orifices that divides and exits as two at the apex;
- Type 6 has two root canals at the orifices, one root canal in the middle and two root canals at the apex;
- Type 7 has one root canal at the orifice that divides and recombines within the body of the root and ends as two root canals; and
- Type 8 has three canals from orifices to apex.

The relationships between root cones, root components and separation structures were analyzed and a canal configuration type application was made for each root component, comparing the number of root cones with the number of root canals along the entire length of each root component. Analyses were performed using the 3D models and the two-dimensional (2D) slices of each root component and in some selected cases, the analysis was supported by using the magnified resin models for verification (Figure 2).

Results

Scanning and segmentation precision

The scanning precision was 6.7 µm ± 10.1 µm (1 SD). The precision of the segmentation was 8.63 µm ± 8.53 µm. After color mapping, the surface models are almost entirely green, reflecting <10 µm distance between the two models (Figures 3A and B).

Qualitative and quantitative morphological analysis of the pulp cavity

The following tooth types were classified into the two groups: a (six maxillary molars, three mandibular molars) and b (five maxillary molars, four mandibular molars). In group a, the largest pulp chambers were associated with no calcified segments. The maxillary palatal root component and the mandibular distal root component were always involved when small areas of mineral deposits were detected, particularly

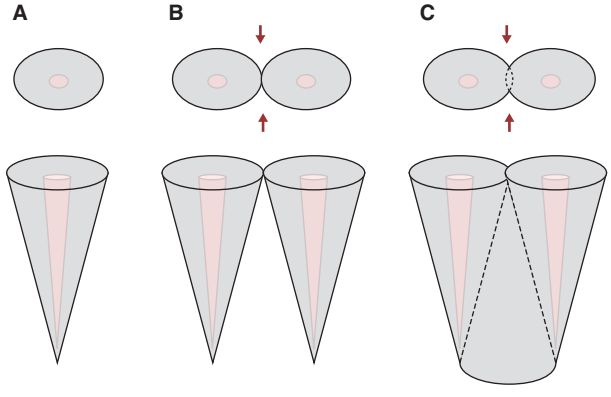

Figure 1. Principal drawings of a root complex comprising one root cone, with a primary main canal (A), a root complex revealing two completely separated root cones each with a primary main canal (B); arrows point to inter-radicular projections. In (C) the root component is composed of two non-separated root cones with two secondary main canals; arrows point to root grooves.

Figure 2. Two different two-colored stereo lithography (stl) models in size 4:1 of a mandibular molar and a maxillary molar. The resin teeth are transparent in light yellow with a dark-brown pulp cavity.

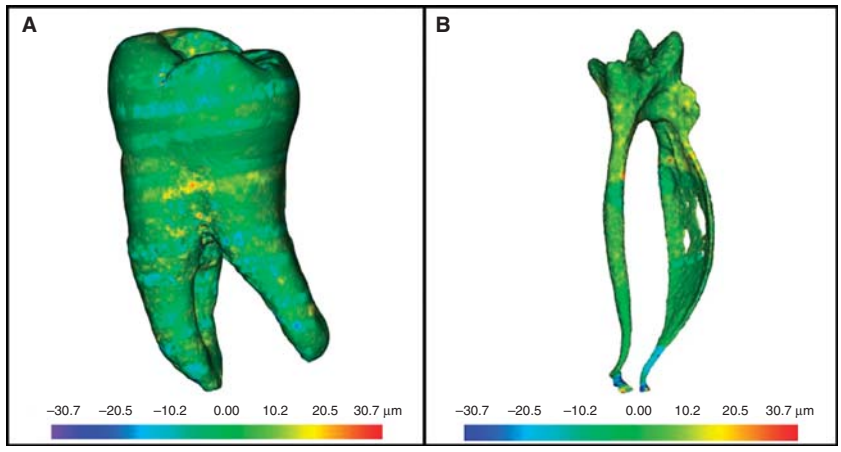

Figure 3. The distance (µm) between two surface models of the same mandibular molar color coded onto one of the models (A). The same method is applied for two different segmentations between surface models of the pulp cavity within the same tooth (B). Positive (red) and negative (blue) distances indicate which of the two models is outside the other.

in the apical region. In one case, calcified segments were covering the canal orifices. In group b, the markedly reduced pulp chambers in the maxillary molars were associated with calcified segments covering the canal orifices, including sporadic accumulation of mineral deposits in the top, middle and apical third of the root canal. However, none of the root canals was completely blocked. In mandibular molars, a larger part of the distal root canals was associated with calcified segments, whereas no calcified segments could be detected in the mesial root components. The mineral deposits were present either as calcified segments connected to the walls of the pulp cavity or as separated objects, as illustrated in the palatal root canal of a maxillary molar (Figures 4A and B). In six of the mandibular molars, intra-radicular connections existed in the mesial root component and eight of the mesiobuccal root components in the maxillary molars had intra-radicular connections. No difference was observed between groups a and b with respect to the presence of intra-radicular connections.

The mb_2 were present in 10 of the maxillary molar teeth. The mean difference in canal length between mb_1 and mb_2 was 0.82 mm with a range of 0.25–1.79 mm. The mb_2 was always shorter than the mb_1.

The principal inter-relation between root canals and root components are illustrated, superimposed with the outlines of each root cone and separation structures, in three transversal planes, in a maxillary molar (Figures 5A–D) and in a mandibular molar (Figures 5E–H). The vast majority of the root components were composed of two root cones and the degree of separation was determined by the manifestation of root grooves. Two non-separated root cones with only superficial root grooves were associated with a broad orifice and the broad outline remained along the entire maxillary palatal root (Figures 5B–D). In principle, the same pattern was seen in the distal root component of the mandibular molar (Figures 5F–G), where the apical transversal plane (Figure 5H) revealed two secondary main canals, basically relating to the two root cones building up the root component. When the root grooves were even more marked, as

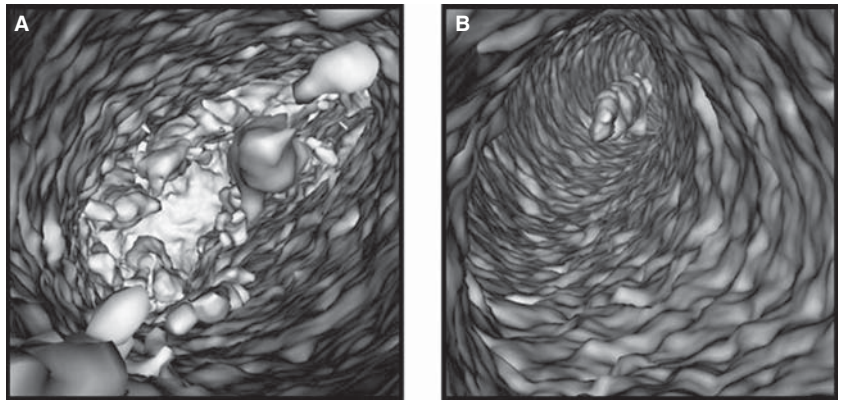

Figure 4. Calcified segments are shown in the palatal root canal (A); the root canal is seen from the pulp chamber. In (B) the root canal is seen from the apex, viewing in the coronal direction; several calcified segments are noted coronally in a palatal root canal.

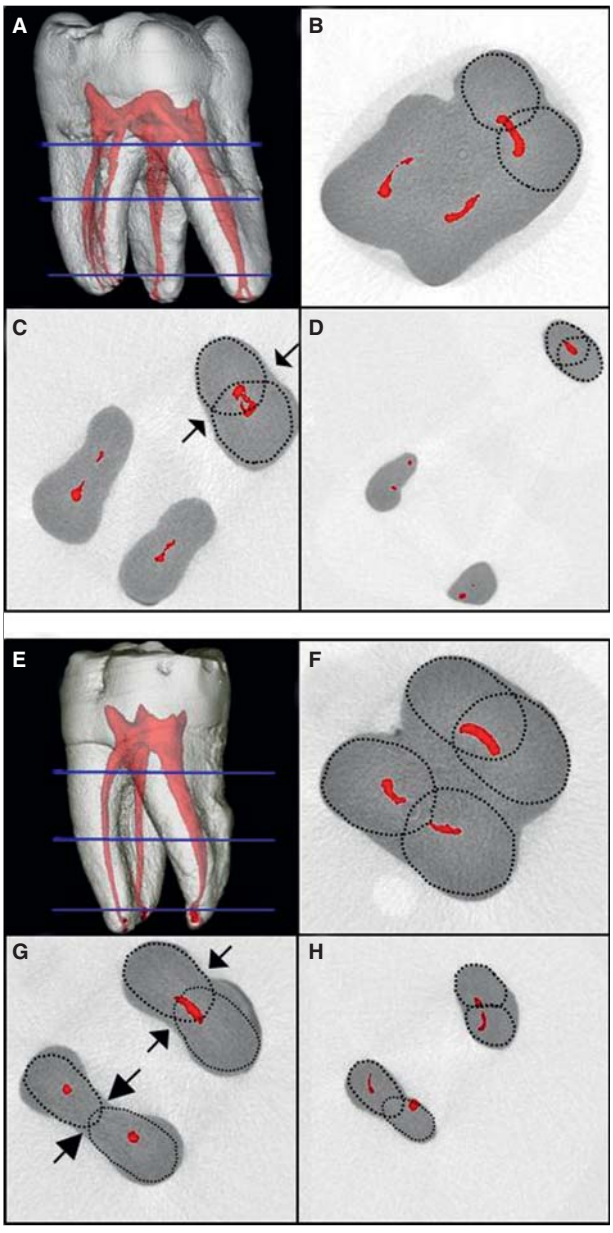

Figure 5. Transparent surface model of a maxillary molar disclosing the pulp cavity (A). Details of three transversal planes along the root complex are illustrated in (B–D). From each plane the relation between root canals and root components are noted and superimposed with the outlines of each root cone. (E) is a transparent surface model of a mandibular molar showing the pulp cavity. As in (A), transversal planes along the root complex (F–H) show the relation between root canals and root components, superimposed with the outlines of each root cone. Arrows indicate separation structures.

illustrated in the mesial root component of the mandibular molar, well-defined circular outlines of both the root cones and the secondary root canals were noted (Figure 5G).

In the mandibular molar teeth, the mesial root components were composed of two root cones, except in one case, where the root component was composed of three root cones. The distal root components showed examples of both one and two root cones. In the maxillary molar teeth, the mesiobuccal root components always consisted of two root cones, whereas the distobuccal and the palatal root component varied between one and two root cones (Table I). The canal configuration of the mesiobuccal root components was most often scored as Type 4 or 6. Only in one tooth (grouped in a), one secondary main canal was noted, and the canal configuration was scored as Type 1 (Table I). This root component consisted of two non-separated root cones and again the orifice of the secondary main canal was relatively broad (Figure 6A).

Discussion

We have created satisfactory 3D surface models of the pulp cavity with a scanning and segmentation precision of <1 voxel. In a similar study, Peters et al. [10] also reported a precision error less than 1 voxel (unit: 39 μm). However, we used a voxel size (unit: 30.7 μm) which corresponds to about half of their voxel volume, reflecting a better resolution in the present study. Even though resolution can be improved further [32] it is a fact that if root canals are smaller than the resolution, the visualization of the root canal will not appear in the surface model. Therefore, quantitative assessments of 3D reconstructed volumes should be interpreted in light of the resolution and the obtained precision [10,33]. In addition, we have applied a new color mapping method for visualization of the precision variation.

We are aware of the limited number of teeth in the present study. However, our inclusion criteria based on the size of the pulp chamber have provided new information. In teeth with relatively small pulp chambers, the number of separated calcified objects was larger in the pulp cavity and the calcified segments were more evenly distributed than observed in presumably younger teeth with relatively larger pulp chambers. Among these teeth we only saw the onset of calcified segments in the apical region, indicating that the calcification of root canals may initiate here. Tidmarsh [28] has previously described changes over time in the pulp chamber, but did not include information about the root complex. The appearance of intra-radicular connections was a common observation in mesial root components in molars and evenly distributed in our material. This may indicate that an intra-radicular connection also denoted an isthmus does not disappear over time, but remains a challenge. Recently, the efficacy of removing debris *in-vitro* from this region was found incomplete [5], confirming the complexity of controlling an infection during the treatment and/or prevention of apical periodontitis.

A review of the literature concerning the frequency of mb_2 has revealed a mean prevalence of 56.8% and with a higher prevalence of mb_2 reported *in vitro* than *in vivo* [20]. We observed a relatively high mb_2

Table I. Vertucci's canal configurations combined with the number of root cones (*n*).

Maxillary molars	Type 1	Type 4	Type 6	Type 7	
Mesiobuccal root component	1 (2)	4 (2)	4 (2)	2 (2)	
Distobuccal root component	6 (1) 4 (2)	—	1 (2)	—	
Palatal root component	4 (1) 7 (2)	—	—	—	
Mandibular molars	Type 1	Type 2	Type 3	Type 4	Type 3-1[a]
Mesial root component	—	1 (2)	1 (2)	3 (2)	1 (3)
Distal root component	6 (2) 1 (1)	—	—	—	—

[a]Gulabivala et al. [36] supplemental canal configurations, three canals joining into one canal.

frequency of 91%, with a root canal length close to the mb_1. However, it should be emphasized that the sample size was relatively small. From a morphological point of view, it is important to perform a straight-line access, with the orifice oriented toward the border between the furcal and pulpal walls prior to mb_2 instrumentation. Clinically the mb_2 is always difficult to negotiate and sometimes difficult to instrument [34,35]. However, as observed in our study, accumulation of mineral deposits may narrow the root canal, but it does not seem to be completely blocked in molar teeth. Therefore, magnification, preferably a microscope, is crucial for successful treatment outcome in such cases, as well as the use of sonic or ultrasonic micro-cutters for the removal of mineral deposits in the pulp cavity [26].

In the present study, we have merged the morphological definitions of Carlsen [21] and the clinical canal classification by Vertucci [15]. We have confirmed that the shape of the orifice matches the outline of the root component [3]. Accordingly, if one (secondary main) root canal with a relatively broad orifice is observed (Figure 6A) and clinically judged as a Type 1 configuration, the root component will always consist of at least two merging root cones. Vertucci's classification system has an important clinical impact [15], but it does not relate the morphology to external macro-morphological structures.

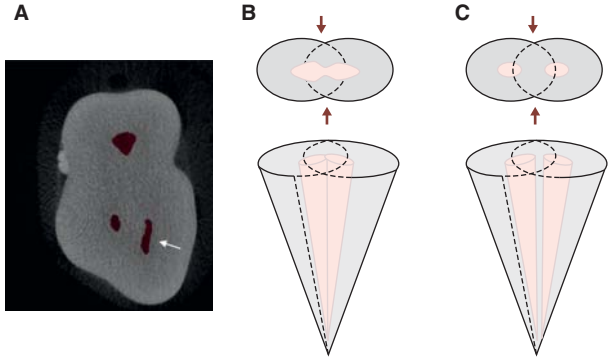

Figure 6. A tomographic slice of a maxillary molar at the orifice level. The white arrow shows the mesiobuccal root component with clinically one root canal but with a broad orifice, as a consequence of two non-separated root cones (A). Principal drawings of (A) showing the two non-separated root cones with one secondary main canal (B). The changes due to mineral deposits laid down over time will modify the internal morphology showing two secondary main canals (C).

The morphological definitions applied in this study simplify the understanding of the composition of the root canal system. The changes due to mineral deposits laid down over time may modify the internal morphology of the tooth (Figures 6B and C) and clinically complicate the endodontic treatment. It could be speculated that the Type 1 configuration found in group a, with a broad orifice, may have the potential to transform into any of the suggested configurations over time, but always on the basis of the composition of the macro morphology. In this context, the creation of two-colored resin models of molar teeth with different morphology represent an excellent educational tool, in the pre- and postgraduate endodontic training of students and dentists, in order to understand the root canal system and its difficulties.

In conclusion, we have made reproducible 3D surface models with a high precision. An increased accumulation of mineral deposits was noted in molars with small pulp chambers and combined with the consistent pattern of intra-radicular connections; the potential endodontic treatment complexity is underlined in such cases. When merging external and internal definitions of the root canal complex, a more detailed understanding of root canal prevalence is reached in varying sizes of the pulp cavity. A future application of our method is to study tissue removal after mechanical preparation in different parts of the root canals, using color mapping.

Acknowledgments

Thanks to Renée Anderson for proofreading.

Declaration of interest: The authors report no conflicts of interest. The authors alone are responsible for the content and writing of the paper.

References

[1] Vertucci FJ. Root canal morphology and its relationship to endodontic procedures. Endod Topics 2005;10:3–29.

[2] Weine FS, Healey HJ, Gerstein H, Evanson L. Canal configuration in the mesiobuccal root of the maxillary first molar and its endodontic significance. Oral Surg Oral Med Oral Pathol 1969;28:419–25.

[3] Bjørndal L, Carlsen O, Thuesen G, Darvann T, Kreiborg S. External and internal macromorphology in 3D-reconstructed maxillary molars using computerized X-ray microtomography. Int Endod J 1999;32:3–9.

[4] Vier-Pelisser FV, Dummer PMH, Bryant S, Marca C, Só MVR, Figueiredo JAP. The anatomy of the root canal system of three-rooted maxillary premolars analysed using high-resolution computed tomography. Int Endod J 2010; 43:1122–31.

[5] Susin L, Liu Y, Yoon JC, Parente JM, Loushine RJ, Ricuccu D, et al. Canal and isthmus debridement efficacies of two irrigant agitation techniques in a closed system. Int Endod J 2010;43:1077–90.

[6] Bergmans L, Cleynenbreugel JV, Wevers M, Lambrechts P. A methodology for quantitative evaluation of root canal instrumentation using microcomputed tomography. Int Endod J 2001;34:390–8.

[7] Nielsen RB, Alyassin AM, Peters DD, Carnes DL, Lancaster J. Microcomputed tomography: an advanced system for detailed endodontic research. J Endod 1995;21:561–8.

[8] Gluskin AH, Brown LS, Buchanan LS. A reconstructed computerized topographic comparison of Ni-Ti rotary GTTM files versus traditional instruments in canal shaped by novice operators. Int Endod J 2001;34:476–84.

[9] Peters OA, Laib A, Göhring TN, Barbakow F. Changes in root canal geometry after preparation assessed by high-resolution computed tomography. J Endod 2001;27:1–6.

[10] Peters OA, Laib A, Rüegsegger P, Barbakow F. Three-dimensional analysis of root canal geometry by high-resolution computed tomography. J Dent Res 2000;6:1405–9.

[11] Peters OA, Schönenberger K, Laib A. Effects of four Ni-Ti preparation techniques on root canal geometry assessed by micro computed tomography. Int Endod J 2001;34:221–30.

[12] Peters OA, Peters CI, Schönenberger K, Barbakow F. ProTaper rotary root canal preparation: effects of canal anatomy on final shape analyzed by micro CT. Int Endod J 2003;36: 86–92.

[13] Peters OA. Current challenges and concepts in the preparation of root canal systems: a review. J Endod 2004;30:559–67.

[14] Gao Y, Peters OA, Wu H, Zhou X. An application framework of three-dimensional reconstruction and measurement for endodontic research. J Endod 2009;35:269–74.

[15] Vertucci FJ. Root canal anatomy of the human permanent teeth. Oral Surg Oral Med Oral Pathol 1984;58:589–99.

[16] Filho FB, Zaitter S, Haragushiku GA, Campos EA, Abuabare A, Correr GM. Analysis of the internal anatomy of maxillary first molars by using different methods. J Endod 2009;35:337–42.

[17] Hartwell G, Bellizzi R. Clinical investigation of *in vivo* endodontically treated mandibular and maxillary molars. J Endod 1982;8:555–7.

[18] Kulid JC, Peter DD. Incidence and configuration of canal systems in the mesiobuccal root of maxillary first and second molars. J Endod 1990;16:311–17.

[19] Somma F, Leoni D, Plotino G, Grand MN, Plasschaert A. Root canal morphology of the mesio-buccal root of maxillary first molars: a micro-computed tomographic analysis. Int Endod J 2009;42:165–74.

[20] Cleghorn BM, Christie WH, Dong CCS. Root and root canal morphology of the human permanent maxillary first molar: a literature review. J Endod 2006;32:813–21.

[21] Carlsen O. Dental Morphology. 1st ed. Copenhagen: Munksgaard; 1987.

[22] Carlsen O, Alexandersen V. Radix mesiolingualis and radix distolingualis in a collection of permanent maxillary molars. Acta Odontol Scand 2000;58:229–36.

[23] Carlsen O, Alexandersen V. Radix paramolaris and radix distomolaris in Danish permanent maxillary molars. Acta Odontol Scand 1999;57:283–9.

[24] Carlsen O, Alexandersen V. Root canals in two-rooted maxillary second molars. Acta Odontol Scand 1997;55:330–8.

[25] Park JW, Lee JK, Ha BH, Choi JH, Perinpanayagam H. Three-dimensional analysis of maxillary first molar mesiobuccal root canal configuration and curvature using microcomputed tomography. Oral Surg Oral Med Oral Pathol Oral Radiol Endod 2009;108:437–42.

[26] Machtou P. The surgical microscope. In: Bergenholtz G, Hørsted-Bindslev P, Reit C, editors. Textbook of endodontology. 2nd ed. Oxford: Wiley-Blackwell; 2009. p 163–8.

[27] Solheim T. Amount of secondary dentin as an indicator of age. Scand J Dent Res 1992;100:193–9.

[28] Tidmarsh BG. Micromorphology of pulp chambers in human molar teeth. Int Endod J 1980;13:69–75.

[29] Darvann T. Landmarker: a VTK-based tool for landmarking of polygonal surfaces. In: Takada K, Kreiborg S, editors. In silico dentistry: the evolution of computational oral health science. Osaka: Medigit; 2008. p 160–2.

[30] Lorensen W, Cline H. Marching cubes: a high resolution 3D surface construction algorithm. Comp Graphics 1987;21: 163–8.

[31] Zhang Z. Iterative point matching for registration of free-form curves and surfaces. Int J Comp Vision 1994;13: 119–52.

[32] Metzger Z, Zary R, Cohen R, Teperovich E, Paqué F. The quality of root canal preparation and root canal obturation in canals treated with rotary versus self-adjusting files: a three-dimensional micro-computed tomographic study. J Endod 2010;36:1569–73.

[33] Dowker SE, Davis GR, Elliott JC. X-ray microtomography: nondestructive three-dimensional imaging for in vitro endodontic studies. Oral Surg Oral Med Oral Pathol Oral Radiol Endod 1997;83:510–6.

[34] Hommez GMG, Braem LM, De Moor RJG. Root canal treatment performed by Flemish dentists. Part 1. Cleaning and shaping. Int Endod J 2003;36:166–73.

[35] Slaus G, Bottenberg P. A survey of endodontic practice amongst Flemish dentists. Int Endod J 2002;35:759–67.

[36] Gulabivala K, Aung TH, Alavi A, Mg Y-L. Root and canal morphology of Burmese mandibular molars. Int Endod J 2001;34:359–70.